

A Reconfigurable Reflector Antenna System With a Hybrid Scanning Method

Imaging antennas for simultaneous multiple spot and wide coverage beams.



On-orbit beam reconfiguration and beam scanning are the two most important features for future satellite antenna payloads. There are several ways of achieving the desired flexibility using different types of antennas and different scanning methods. This article presents single- and dual-reflector antenna systems where reconfiguration is achieved using high-gain multiple beams (HGMBs) employing imaging reflector configurations. Beam scanning over the global coverage is achieved using a combination of precise electronic scanning over a small coverage region and a coarse mechanical scanning over a wide global coverage. This method results in significant improvement in gain relative to conventional

methods that employ element beams and can simultaneously provide both HGMBs and wide-area coverage beams with low-cost payloads.

BACKGROUND

There is a need for on-orbit beam reconfiguration and beam scanning for satellite antennas used for communications satellite payloads. This is required for operational flexibility involving changes in coverage, beam scanning, and interference mitigation. Types of antennas that could provide the desired on-orbit flexibility include:

- phased-array antennas (PAAs)
- confocal reflector antennas (CRAs)
- focal-plane reflector antennas (FPRAs)
- single- or dual-reflector imaging antennas (SRIAs/DRIAs).

Most of the aforementioned antenna systems have been described in the past [1]–[3]. For high-gain applications, the number of elements using PAAs becomes extremely large (of approximately several tens of thousands) and thus becomes impractical. However, PAAs have the advantage of providing electronic scanning for medium-gain antennas [4]. A CRA is similar to a PAA, but it employs a parabolic subreflector and a parabolic main reflector with a common focal point, and the subreflector is fed with a phased array [3]. The phased array of a CRA needs to scan M times the desired beam scan (M being the magnification of the confocal antenna defined as the ratio of the focal lengths of main reflectors and subreflectors, $M > 1$). A CRA also requires a number of elements similar to

a PAA with spacing M times smaller, and it has the additional complexity of a large main reflector, subreflector, and a flat plate with a hole to eliminate the grating lobes. This system is not practical, although several theoretical studies were conducted and prototypes are being built, and there are no satellite systems in space currently that employ CRAs.

FPRA, either single or dual, have the feed array located in the focal plane of the reflector. An FPRA requires electrically small feeds (approximately one wavelength size) to get good adjacent beam overlap. Because of small feed size, the reflector (or subreflector in a dual-reflector system) is not optimally illuminated. Hence, the antenna efficiency is very low (approximately 50%) [1]. Also, the beams do not combine well if a large area beam needs to be formed.

Scan performance of an offset dual-reflector Gregorian antenna is shown by Akigawa and Di Fonzo [5] for small scan angles. Improved scan performance was achieved by shaping the reflector surfaces as described in [6] by Albertson et al. To achieve low scan losses, offset hyperbolic subreflectors with concave shapes (instead of conventional convex hyperboloids) that are confocal with offset paraboloidal main reflectors were described [7], [8]. Low scan losses of more than 10 beamwidths of scan can be achieved with these systems that are known as *side-fed offset Cassegrain* and *front-fed offset Cassegrain antennas*. Chang and Prata referred to these antennas as *Dragonian reflectors* and provided a step-by-step design procedure based on geometrical optics [9]. A disadvantage of these antennas is that the subreflectors are as big as main reflectors, posing accommodation and mass issues for spacecraft applications.

Bifocal reflectors have been reported [10], [11] where the scan loss is reduced by shaping the dual-reflector system optimized over the scan region between the two foci. This will be useful when the scan region is moderate, unlike the

global coverage, where the beams need to be reconfigured over several tens of beamwidths. Nuria Llombart [12], [13] proposed a confocal ellipsoidal Gregorian reflector system in which the main reflector is an ellipsoid, the subreflector is a paraboloid, and a rotating mirror was used to scan the beams at terahertz frequencies. A non-focusing antenna system using a convex hyperboloid was reported to generate multiple beams using a single feed per beam [14]. This system has limited scan capability and also suffers from reduced gain relative to other systems.

A design procedure for a multireflector multiple-beam antenna where the coverage is fixed is given in [15] using either three or four offset parabolic reflector antennas. A stepped-reflector antenna system for multibeam and multiband applications is

reported where a small annular step is introduced to the surface of the to create approximately the same beam size at both uplink receive and downlink transmit bands [16]. This system reduces the number of reflectors by half by using dual-band feeds to generate fixed overlapping beams over a given geographical coverage as seen from a satellite. For large scan coverages, several design improvements were reported that included using a large focal-length-to-diameter ratio, shaping the reflector surface based on improving scan loss for edge beams, using a curved feed array (instead of planar), and having three or seven feed elements to improve scanned beam performance at the edge of the coverage region [17].

Antenna systems that are suitable for these applications are the SRIA or the DRIA. These systems were not exploited to their maximum potential to date. This article presents flexible antennas that can produce multiple element beams and a larger coverage beam simultaneously. Multiple quiescent beams are used to create an adapted beam that can null a number of interferers or to provide higher gain spot beams. The antenna beams are scanned together maintaining the adjacent beam overlap over global coverage regions using a hybrid scanning method with electronic scanning of the feed array over a smaller coverage and mechanical scanning of the main reflector with a fixed feed array and subreflector over a larger coverage region. Both the SRIA and DRIA exemplary designs are presented along with computed results. The extension of these designs to multiple frequency bands as well as future trends are discussed along with impacts on feed assembly and associated hardware.

SRIA

The feed array in an imaging reflector antenna is displaced from the focal plane, usually toward the main reflector to make it compact. This will broaden the element beam and improve

The use of HGMBs allows interference cancellation from several jammers and also enables the formation of a large theater coverage.

the adjacent beam overlap, allowing the use of a large number of element beams to form HGMBs with improved gain. Improvement in gain is achieved due to optimal illumination on the reflector when compared to a single-element beam. The HGMBs can be electronically scanned over a small theater coverage. The use of HGMBs allows interference cancellation from several jammers and also enables the formation of a large theater coverage.

Figure 1 shows a schematic of the SRIA. The antenna geometrical parameters are $D = 129 \lambda$, $F/D = 1.2$, and $H = 51.65 \lambda$, where λ is the wavelength at the midband of low frequency. The feed

The use of HGMBs instead of element beams provides much better gain-to-noise-temperature on the uplink or better effective isotropic radiated power on the downlink.

array is defocused by a certain distance from the focal point toward the main reflector aperture center ($h = 5.17 \lambda$) to create imaging optics in the far field. As a result, the element beams broaden, depending on the defocus distance, resulting in an increased overlap between adjacent beams. Element beams typically have lower gain due to nonoptimal illumination on the reflector. By combining a number of element beams, a certain number of HGMBs are formed, and these HGMBs are then used to form either an adapted beam

creating nulls in the location of interferers or a theater coverage with higher gain. The use of HGMBs instead of

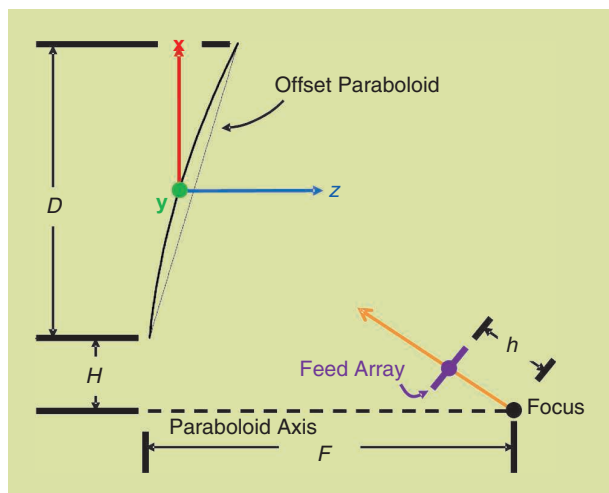


FIGURE 1. A schematic of the SRIA with a feed array located in the image plane.

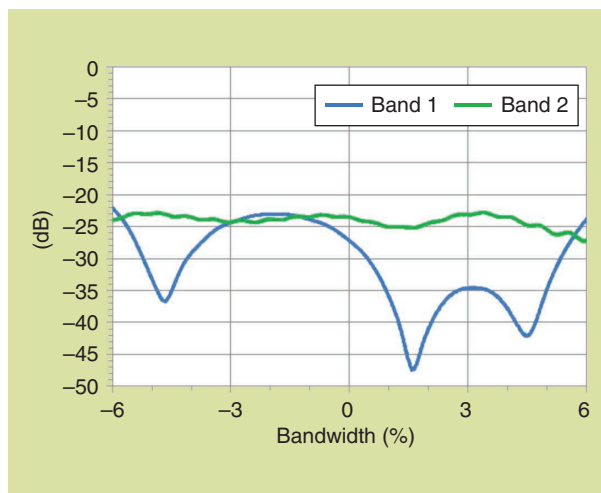


FIGURE 3. The measured reflection coefficient (S11) of the integrated feed assembly at both bands.

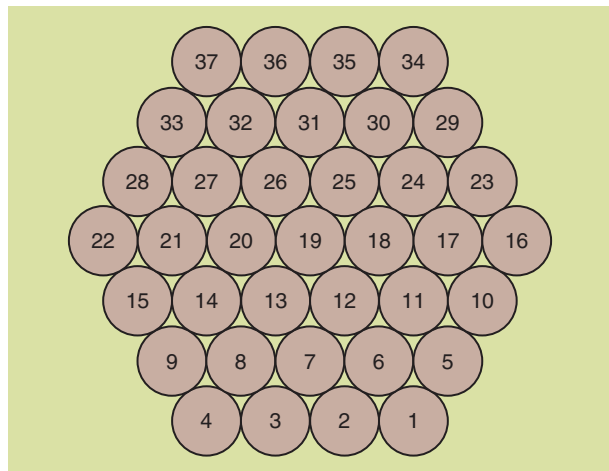


FIGURE 2. A feed-array hexagonal grid layout for the SRIA.

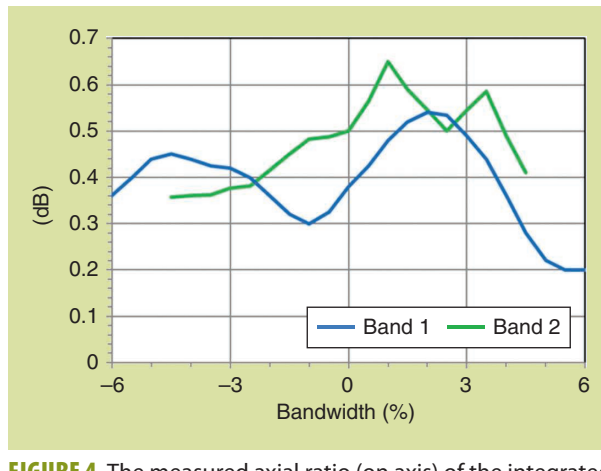


FIGURE 4. The measured axial ratio (on axis) of the integrated feed assembly at both bands.

element beams provides much better gain-to-noise-temperature (G/T) on the uplink or better effective isotropic radiated power (EIRP) on the downlink.

The feed array for an imaging antenna is shown in Figure 2. The 37 elements of the array are arranged in a hexagonal lattice to achieve better overlap among adjacent beams. The element diameter (d) depends on the F/D ratio of the reflector antenna and is typically given as

$$d/\lambda = C(F/D), \quad (1)$$

where C is a constant and is in the range of 1.1–1.25 depending on the application [18].

Feed horns suitable for feed arrays are either multi-flare smooth-walled horns for wideband and multiband applications or Potter horns for narrow-band applications.

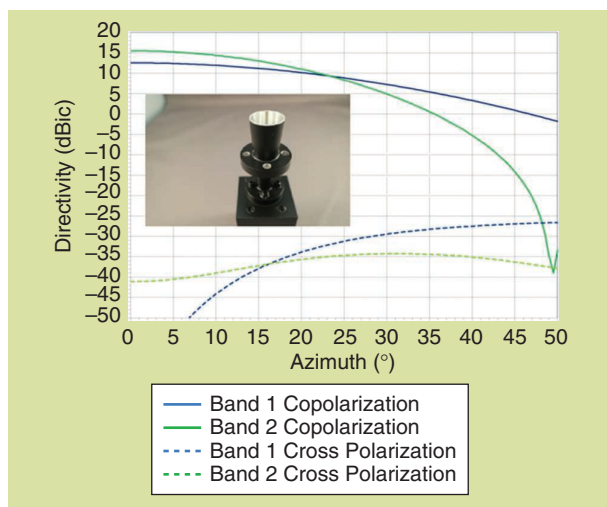


FIGURE 5. The measured feed patterns at low and high bands. The feed assembly fabricated is shown as the inset.

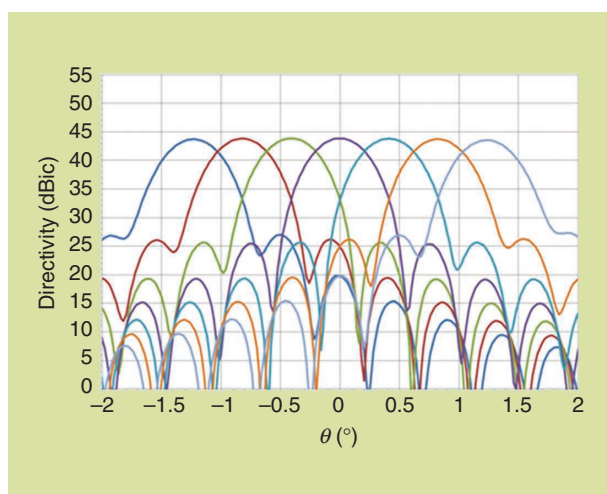


FIGURE 6. Computed element beam patterns of SRIA in azimuth plane, where each beam is generated with single feed horn.

Corrugated horns are not suitable for these applications due to thick walls to accommodate the corrugations, and they have the disadvantages of low efficiency and poor overlap among adjacent beams. The feed assembly is designed to operate over dual bands separated by a factor of 1.6 (center frequencies of high-band and low-band ratio) with an overall bandwidth of 20.5% with dual-circular-polarization (CP) capability at both bands. The feed assembly comprises a multiflare horn [6] with an aperture diameter of 1.19λ at the low band (band 1), a polarizer, and filters to isolate the two bands with more than 50-dB isolation.

The measured return loss of the integrated feed assembly at both bands is shown in Figure 3, and the axial ratio measurements are depicted in Figure 4. The percentage bandwidths for low (band 1) and high (band 2) are $\pm 1.7\%$ and $\pm 2.5\%$, respectively, from the center frequency of

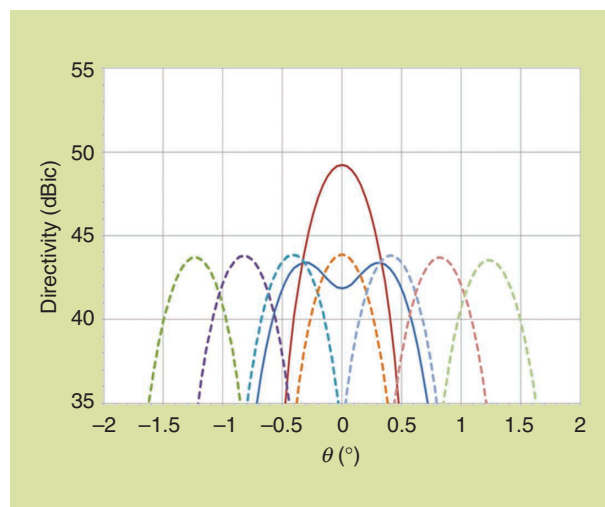


FIGURE 7. Moderate gain beams formed by combining low-gain element beams using a passive BFN.

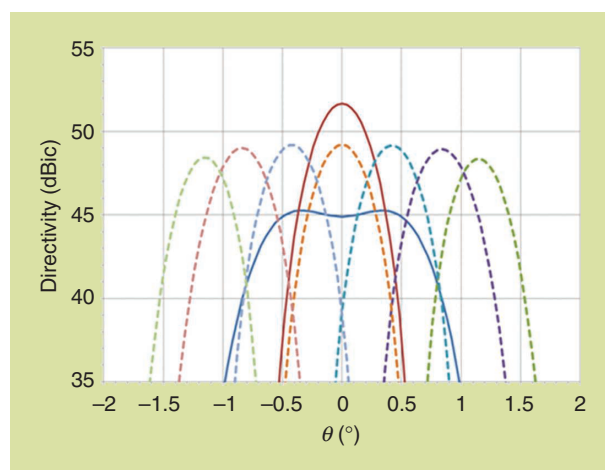


FIGURE 8. MGMBs along the azimuth plane are used to synthesize the high-gain spot beam as well as a 1° coverage beam with much higher gain values compared to conventional designs (band 1).

each band. The measured return loss is better than 23 dB, and the measured axial ratio is better than 0.65 dB at both bands. The feed-element patterns measured in an anechoic chamber are given in Figure 5 showing excellent cross-polarization performance at both bands. The feed assembly fabricated is shown as an inset in Figure 5. The measured feed patterns are used to compute the SRIA secondary-element beam patterns (defined as a single feed illuminating the main reflector of the SRIA) in the azimuth plane. Note that the antenna system described here is for future satellite programs; hence, the reflector is not fabricated.

The complete antenna system will be manufactured, tested, and space qualified in the near future. However, the secondary patterns are simulated using measured feed patterns and computing using TICRA's GRASP commercial software [19], which is proven to be accurate. The seven beams in the azimuth plane at band 1 are plotted in Figure 6 showing good adjacent beam overlap but with a low efficiency of 14%. This is due mainly to a low illumination taper of approximately 2.2 dB on the reflector edge (see Figure 6). Figure 7 shows a single high-gain beam at the boresight and an area coverage beam obtained by combining the array elements through a passive beamforming network (BFN). The on-axis gain for the boresight beam has improved to 49.2 dBic, resulting in a moderate efficiency of 50.6%. The associated area beam (1° in diameter) by combining all of the 37 element beams with appropriate amplitude and phase distribution is shown as the solid blue curve, with a minimum directivity of 42.2 dBic. This is a conventional approach.

A compact DRIA using a center-fed Gregorian antenna is used at GPS bands to provide beam flexibility at L1, L2, and L5 bands, covering approximately 31% of bandwidth.

Now we show that, by combining several of the medium gain multiple beams (MGMBs) (as shown by the red curve of Figure 7), HGMBs can be generated, as shown in

Figure 8. These beams are realized with a digital BFN to synthesize a high-gain spot beam with a 51.4-dBic gain, representing an efficiency of about 80%. This efficiency is theoretically the maximum that could be achieved with a reflector antenna. The gain increase is approximately 2.2 dB compared to conventional designs, and this increase is possible due to illuminating the reflector with optimal illumination and improving the beam overlap among adjacent beams.

The coverage beam also has a significant increase in gain of

approximately 2.8 dB compared to conventional methods, and it has a minimum directivity of 45.5 dBic over the 1° diameter, as displayed in Figure 9. This represents a gain area product of 24,837, which is the highest possible for a contoured beam [20]. This is due to flat gain over the coverage and a sharp fall off outside of the coverage region. Figure 10 shows scanned beam performance when all beams are scanned by 0.5° and synthesized. This is achieved due to electronic scanning of the feed array of the SRIA. The scan loss is approximately 1 dB and is shown in both the synthesized high-gain spot beam and coverage beam. All of the HGMBs can be utilized to mitigate multiple interferers and provide communication links to most of the coverage region.

At the high band (band 2), the synthesized performance using the dual-band feed array and plots of the HGMBs, spot beam, and coverage beams similar to those presented in Figure 8, is shown in Figure 10. The HGMBs overlap

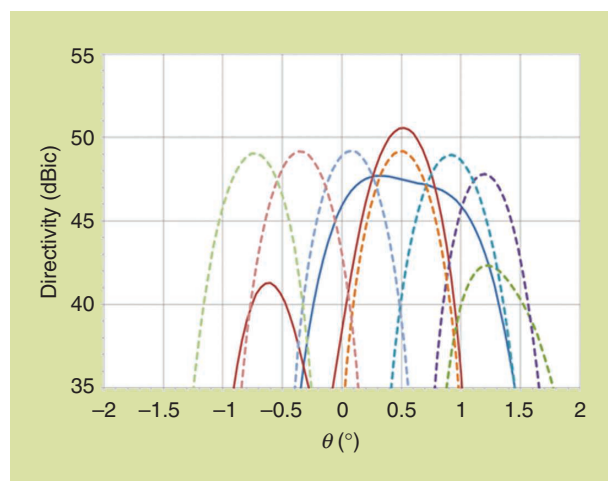


FIGURE 9. MGMBs are used to synthesize a scanned spot beam as well as a scanned coverage beam while still achieving high-gain values for both types of beams (band 1).

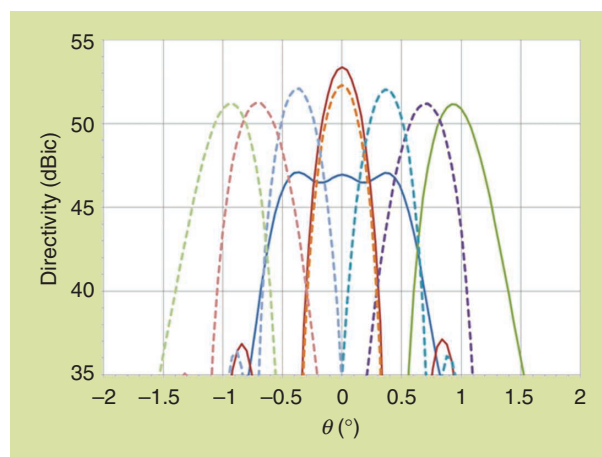


FIGURE 10. MGMBs along the azimuth plane are used to synthesize a spot beam as well as a 1° coverage beam with much higher-gain values compared to conventional designs (band 2).

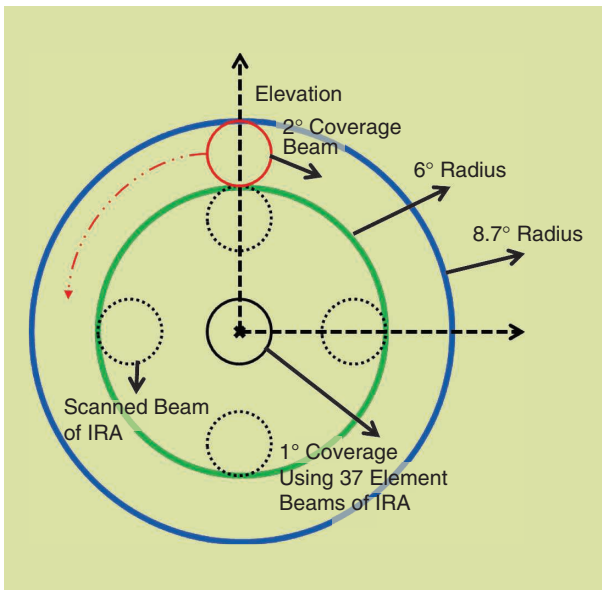


FIGURE 11. An illustration of a hybrid scanning method using mechanical and electronic scanning for wide coverages. IRA: imaging reflector antenna.

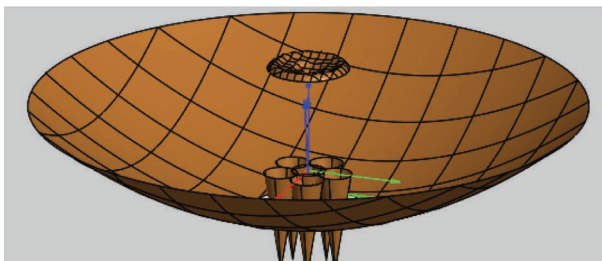


FIGURE 12. The DRIA geometry for the L band.

well, allowing the formation of the spot beam's and coverage beams' increased gain values. For wide scan requirements, such as global coverage, the main reflector is gimbaled using a two-axis gimbal mechanism while keeping the feed array stationary, and then electronic scanning of the feed array is used to fine-tune the location of beams on the ground. This concept is illustrated in Figure 11, where electronic scanning over a 1° area is used to fine-tune the beam location, while coarse scanning over a large coverage region is achieved by mechanical scanning of the reflector. This method minimizes the scan loss while reducing the cost by using only a small feed array with 37 elements.

DRIA

In 1986, Dragone described basic dual-reflector imaging systems using Cassegrainian and Gregorian geometries [20]. However, not much has been done in this area regarding practical implementations of these antennas. A compact DRIA using a center-fed Gregorian antenna is used at GPS bands to provide beam flexibility at L1, L2, and L5 bands, covering approximately 31% of bandwidth. A DRIA employs a 4-m deployable mesh reflector and a shaped elliptical

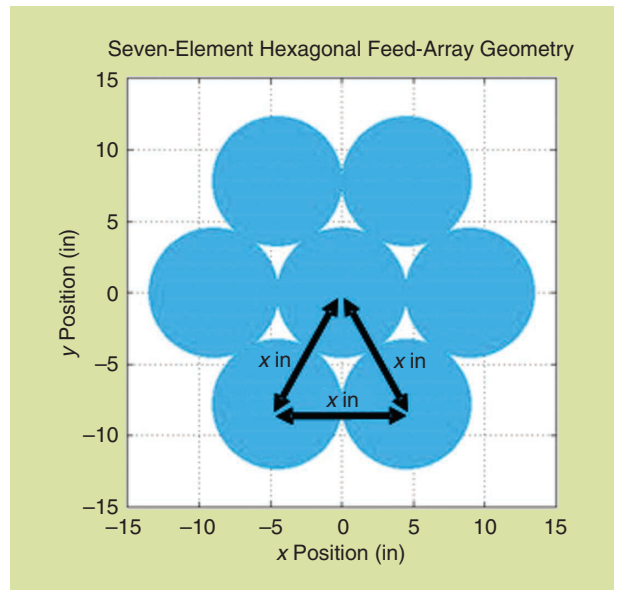


FIGURE 13. A feed layout using a septet array ($x = 8$ in).



FIGURE 14. An integrated radiating element with a low-loss triplexer.

subreflector of a 0.6-m diameter. The DRIA geometry is shown in Figure 12. The feed array comprises a novel seven-element array of a stepped aperture integrated radiator (STAIR) [21].

Each element has a 7.5-in diameter and is integrated with a compact triplexer that separates each of the three bands with high isolation. The elements are arranged in a hexagonal grid to improve the adjacent beam overlap. The feed array (displayed in Figure 13) is defocused by 7.5 in toward the subreflector to improve the adjacent beam overlap needed to synthesize a global coverage beam. The STAIR element with a triplexer is fabricated and is shown in Figure 14. A passive intermodulation (PIM)-free honeycomb panel is used as an interface between the radiating element and the triplexer, depicting the ground plane of the larger array.

TABLE 1. THE L-BAND FEED ASSEMBLY PERFORMANCE.

Parameter	Unit	Performance
Frequency band 1	MHz	1,558–1,594
Frequency band 2	MHz	1,211–1,245
Frequency band 3	MHz	1,163–1,191
Passive intermodulation with TX1: 25 W at 1,243 MHz (band 2); TX2: 44 W at 1,575 MHz (band 1); and RX: 332 MHz	dBm	PIM < -130
Polarization	—	RHCP
Return loss	dB	19
Insertion loss, band 1	dB	0.45
Insertion loss, band 2	dB	0.47
Insertion loss, band 3	dB	0.54
Rejection	dB	>45 dB among bands
Axial ratio	dB	<1 dB
Aperture efficiency	%	95
Power handling, average	W	88 (average)
Minimum multipaction margin to 88 W	dB	13
RF interface	—	TNC female
Temperature range	°C	-20 to +100

RHCP: right-hand CP; TX1: transmit channel 1; TX2: transmit channel 2; Rx: receive; TNC: threaded navy connector.

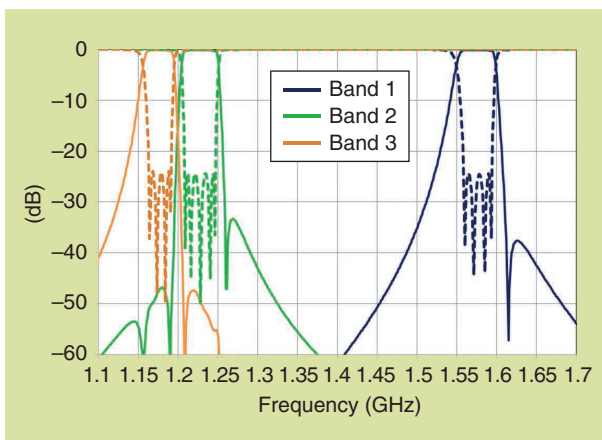


FIGURE 15. The triplexer performance.

The measured radio-frequency (RF) performance of the integrated element with the triplexer is summarized in Table 1. A minimum efficiency of 95% has been measured for the STAIR element, and the integrated element and triplexer show excellent power handling, with a minimum multipaction margin of 13 dB. The insertion loss measured to be 0.54 dB

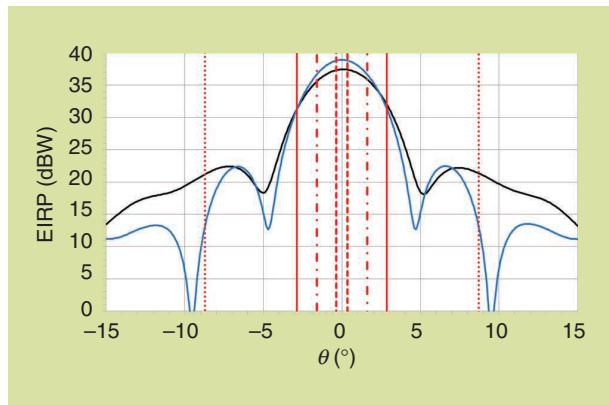


FIGURE 16. The normalized EIRP plots of the DRIA at L1 and L2 bands for the boresight beam.

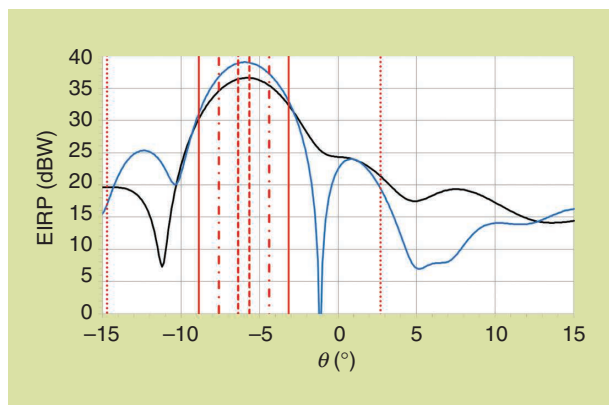


FIGURE 17. The normalized EIRP plots of the DRIA at L1 and L2 bands of the scanned beam.

in the worst-case scenario. The phase center is stable over the band within 0.1 in, resulting in a very low group-delay variation over the frequency bands, an important parameter for navigational payloads. Triplexer performance covering the three bands is plotted in Figure 15 presenting better than 45-dB isolation among the bands. Comb-line filters are employed in the triplexer to keep the geometry compact while achieving the desired isolation and frequency response with minimal insertion loss.

Computed radiation patterns of the DRIA at the L1 and L2 bands are shown in Figure 16. The results are exhibited in normalized EIRP where each element has 1 W of output power. The scanned beam performance shown in Figure 17 is achieved by optimizing the phase excitations of the feed array. In this case, the beam is scanned to 6° from the boresight, with a moderate scan loss of approximately 0.6 dB. A broader beam suitable for larger coverage, such as a global beam, can be synthesized by changing phase distribution of the outer elements relative to the central element. Gain plots are shown in Figure 17, where the beam broadens, and minimum gain over the coverage is approximately 12.5 dBi. A flat beam can also be synthesized (see Figure 18), which requires a larger reflector, a larger feed array of 19 elements, or both.

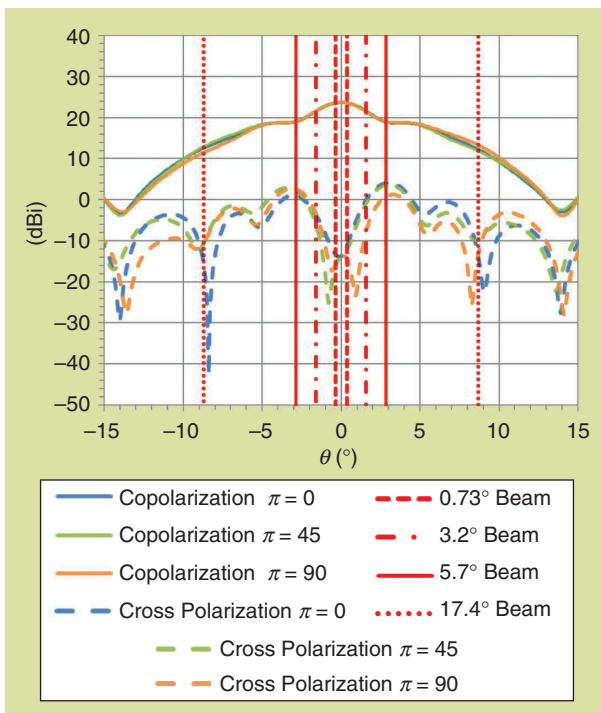


FIGURE 18. The synthesized gain plots of the DRIA at L1 for a wide coverage beam (global) using phase-only optimization.

SUMMARY AND CONCLUSIONS

The use of imaging reflector antennas for beam reconfiguration with a small feed array is discussed in this article. An SRIA using a 37-element array is shown to provide the required beam flexibility while providing high-gain values using HGMBs. This approach will provide an improvement of approximately 2.2 dB compared to conventional approaches due to efficient illumination on the reflector and better overlap among the element beams. The number of elements can be reduced significantly by using a hybrid scanning method with electronic scanning of the feed array over a small coverage combined with coarse scanning over larger coverage by gimbaling the reflector with a fixed feed array. A dual-reflector imaging antenna at the L band with a seven-element array is shown to provide the required on-orbit beam flexibility by phase-only synthesis. The proposed method has the advantages of realizing high-gain multiple and shaped beams over a large coverage region using low-cost imaging reflector antenna designs. The beam locations and shapes can be reconfigured on orbit using digital beamforming or a combination of analog and digital beamformers, depending on the applications.

AUTHOR INFORMATION

Sudhakar K. Rao (skraoks@yahoo.com) is a technical fellow at Northrop Grumman Aerospace Systems, Redondo Beach, California. His research interests include antenna systems for space, air, and ground applications. He is a Life Fellow of the IEEE.

Philip Venezia (venezia@custommicrowave.com) is the director of the Innovation Center of Excellence at Custom Microwave Inc., Longmont, Colorado. His research interests

include reflector antennas, multifrequency antenna feeds, and extremely high-performance passive waveguide components for use in the space industry.

Clency Lee-Yow (clency@custommicrowave.com) is the president and chief executive officer of Custom Microwave Inc., Longmont, Colorado. His research interests include developing antenna products for space applications.

REFERENCES

- [1] S. Rao, "Advanced antenna technologies for satellite communications payloads," *IEEE Trans. Antennas Propag.*, vol. 63, no. 4, pp. 1205–1217, 2015. doi: 10.1109/TAP.2015.2391283.
- [2] C. Babu Ravipati and S. Rao, "Advanced reflector antennas," in *Handbook of Reflector Antennas and Feed Systems*, vol. 1, S. K. Sharma, S. Rao, and L. Shafai, Eds. Norwood, MA: Artech House, 2013, pp. 219–246.
- [3] C. Dragone and M. J. Gans, "Imaging reflector arrangements to form a scanning beam using a small array," *Bell Syst. Tech. J.*, vol. 58, no. 2, pp. 501–515, 1979. doi: 10.1002/j.1538-7305.1979.tb02230.x.
- [4] S. Rao, M. Tang, and C.-C. Hsu, "Multiple beam technology for satellite communications payloads," *Appl. Comput. Electromagn. Soc. J.*, vol. 21, no. 3, pp. 353–364, 2006.
- [5] M. Akagawa and D. DiFonzo, "Beam scanning characteristics of offset Gregorian antennas," in *Proc. 1979 Antennas and Propagation Society Int. Symp.*, pp. 262–265.
- [6] N. Albertsen, K. Pontoppidan, and S. Sorensen, "Shaping of dual reflector antennas for improvement of scan performance," in *Proc. 1985 Antennas and Propagation Society Int. Symp.*, pp. 357–360.
- [7] S. Makino, Y. Kobayashi, and T. Katagi, "Front fed offset Cassegrain type multibeam antenna," in *Proc. 1985 Antennas and Propagation Society Int. Symp.*, pp. 341–344.
- [8] R. Jorgensen, P. Balling, and W. English, "Dual offset reflector multibeam antenna for international communications satellite applications," *IEEE Trans. Antennas Propag.*, vol. 33, no. 12, pp. 1304–1312, 1985. doi: 10.1109/TAP.1985.1143523.
- [9] S. Chang and A. Prata, "The design of classical offset Dragonian reflector antennas with circular apertures," *IEEE Trans. Antennas Propag.*, vol. 52, no. 1, pp. 12–19, 2004. doi: 10.1109/TAP.2003.822435.
- [10] B. L. Rao, "Bifocal dual reflector antenna," *IEEE Trans. Antennas Propag.*, vol. 22, no. 5, pp. 711–714, 1974. doi: 10.1109/TAP.1974.1140869.
- [11] M. E. Lorenzo, C. M. Rappaport, and A. G. Pino, "A bifocal reflector antenna with Gregorian configuration," in *Proc. IEEE Antennas and Propagation Society Int. Symp. 1996 Dig.*, vol. 1, pp. 234–237.
- [12] N. Llombart, K. Cooper, R. J. Dengler, T. Bryllert and P. H. Siegel, "Confocal ellipsoidal reflector system for a mechanically scanned active terahertz imager," *IEEE Trans. Antennas Propag.*, vol. 58, no. 6, pp. 1834–1841, 2010. doi: 10.1109/TAP.2010.2046860.
- [13] N. Llombart, R. Dengler, and K. Cooper, "Terahertz antenna system for a near-video-rate radar imager," *IEEE Antennas Propag. Mag.*, vol. 52, no. 5, pp. 251–259, 2010. doi: 10.1109/MAP.2010.5687559.
- [14] P. Ingerson and C. Chen, "The use of non-focusing aperture for multibeam antenna," in *Proc. 1983 Int. Antennas and Propagation Society Int. Symp.*, pp. 330–333.
- [15] S. K. Rao, "Design and analysis of multiple-beam reflector antennas," *IEEE Antennas Propag. Mag.*, vol. 41, no. 4, pp. 53–59, 1999. doi: 10.1109/74.789737.
- [16] S. K. Rao and M. Q. Tang, "Stepped-reflector antenna for dual-band multiple beam satellite communications payloads," *IEEE Trans. Antennas Propag.*, vol. 54, no. 3, pp. 801–811, 2006. doi: 10.1109/TAP.2006.869938.
- [17] P. Ramanujam and L. R. Fermelia, "Recent developments on multi-beam antennas at Boeing," in *Proc. 8th European Conf. Antennas and Propagation*, 2014, pp. 405–409.
- [18] S. Rao and C. B. Ravipati, "Reflector antennas for space communications," in *Handbook of Reflector Antennas and Feed Systems*, vol. 3, S. K. Sharma, S. Rao, and L. Shafai, Eds. Norwood, MA: Artech House, 2013, pp. 13–76.
- [19] TICRA, Copenhagen, Denmark. *GRASP User's Manual, Version 10.6.0*. (2017). [Online]. Available: <http://www.ticra.com>
- [20] C. Dragone, "Theory of imaging in Cassegrainian and Gregorian antennas," *IEEE Trans. Antennas Propag.*, vol. 34, no. 5, pp. 689–701, 1986. doi: 10.1109/TAP.1986.1143870.
- [21] S. Rao, C. Lee-Yow, P. Venezia, and J. Scupin, "L-band array element with integrated triplexer for GPS payloads," U.S. Patent 9972897, May 15, 2018.